PHYSICAL REVIEW B **78**, 180402(R) (2008)

Influence of oxidation on the spin-filtering properties of $CoFe_2O_4$ and the resultant spin polarization

A. V. Ramos,[1] T. S. Santos,[2,3] G. X. Miao,[3] M.-J. Guittet,[1] J.-B. Moussy,[1] and J. S. Moodera[3]
[1]*CEA-Saclay, IRAMIS, SPCSI, 91191 Gif-Sur-Yvette, France*
[2]*Argonne National Laboratory, Argonne, Illinois 60439, USA*
[3]*Francis Bitter Magnet Laboratory, Massachusetts Institute of Technology, Cambridge, Massachusetts 02139, USA*

(Received 24 July 2008; revised manuscript received 14 October 2008; published 5 November 2008)

We report the direct measurement of spin polarization in epitaxial $CoFe_2O_4$ tunnel barriers using the Meservey-Tedrow technique. By observing an asymmetry in the Al quasiparticle density of states in Pt(111)/$CoFe_2O_4$(111)/γ-Al_2O_3(111)/Al tunnel junctions, we prove the existence of spin filtering in our $CoFe_2O_4$ tunnel barriers. We further analyze the effect of oxidation conditions during film growth on the polarization of the tunneling current, revealing an important role played by oxygen vacancies in the spin-filter efficiency of this material.

DOI: 10.1103/PhysRevB.78.180402 PACS number(s): 75.47.Pq, 72.25.−b, 85.75.−d, 73.43.Jn

Spin-polarized tunneling (SPT) across magnetic insulators is of great interest due to their potential integration into devices involving spin injection into semiconductors,[1] tunneling magnetoresistance (TMR),[2] and spin detection.[3] Because of the exchange splitting of the conduction band of a magnetic insulator, there exist two distinct tunnel barrier heights for spin-up and spin-down electrons, leading to the spin-selective transport of electrons, and hence a large spin polarization can result. This effect, known as spin filtering, may be directly measured by the Meservey-Tedrow technique[4] which uses a superconducting electrode as the spin analyzer in metal/magnetic insulator/superconductor (SC) tunnel junction. Spin filtering was first demonstrated by the Meservey-Tedrow technique in EuS tunnel barriers[5,6] and followed by the work with EuSe (Ref. 7) and EuO (Ref. 8) barriers. The slightly more complex oxides $BiMnO_3$ (Ref. 9) and $NiFe_2O_4$ (Refs. 10 and 11) have also shown spin-filter capabilities by producing significant TMR effects in magnetic tunnel junctions (MTJs) (Ref. 12) at low temperature.

The ultimate goal in spin filtering is to measure the effect at room temperature.[13] One of the excellent candidates to realize this is $CoFe_2O_4$, whose high Curie temperature (T_C =793 K) and good insulating properties make it a potential candidate for room-temperature spin filtering. Local spin-density approximation calculations using the self-interaction correction predict a lower tunnel barrier height for spin-down electrons and thus negatively polarized spin filtering.[14] Furthermore, spin filtering should be very efficient due to the large exchange splitting of 1.28 eV predicted in the conduction band. Experimentally, we recently showed that $CoFe_2O_4$ is indeed capable of filtering spin at room temperature via TMR measurements in fully epitaxial Pt/$CoFe_2O_4$/γ-Al_2O_3/Co MTJs.[15] The TMR experiments revealed a $CoFe_2O_4$ spin filter that was negatively polarized with a spin-filter efficiency (P_{SF}) of −25% at low temperature. This value was extracted indirectly using the Jullière formula[16] and taking the polarization of the Co counterelectrode to be +40%. In the present work, we use the Meservey-Tedrow technique with a superconducting Al spin analyzer to directly determine P_{SF} and thus show the influence of oxidation conditions in our $CoFe_2O_4$ tunnel barriers on P_{SF}.

$CoFe_2O_4$(111)/γ-Al_2O_3(111) epitaxial double tunnel barriers were grown in ultrahigh vacuum (UHV) conditions at 450 °C by molecular-beam epitaxy (MBE) using a radio-frequency oxygen plasma as the source of atomic oxygen. The films were deposited on α-Al_2O_3(0001) substrates covered with a 20-nm-thick buffer layer of Pt(111) using Knudsen cells for Co, Fe, and Al, and reactively evaporated. Samples were fabricated using different oxygen partial pressures in the plasma source (P_{O_2}), ranging from P_{O_2}=0.2 to 0.4 Torr during growth. These corresponded to an oxygen pressure inside the evaporation chamber of 1.9×10^{-8} to 1.0×10^{-7} Torr. We chose to perform SPT measurements on $CoFe_2O_4$(111) capped with γ-Al_2O_3(111) in order to reproduce the exact tunnel barrier as in our $CoFe_2O_4$-based MTJs.[15] Also, the γ-Al_2O_3 layer served to protect $CoFe_2O_4$ from exposure to air when samples were transported from the MBE chamber to the thermal evaporation chamber used to deposit Al electrodes.

Figures 1(a) and 1(b) show the *in situ* RHEED patterns along $[1\bar{1}00]$ (in the hexagonal coordinate basis of the sapphire substrate) of a $CoFe_2O_4$/γ-Al_2O_3 barrier at two different stages of growth. Both layers display fully epitaxial, two-dimensional quality with the characteristic RHEED patterns of a single-crystalline spinel film. Figure 1(c) shows the Fe 2p and Co 2p XPS peaks, also *in situ*, of a $CoFe_2O_4$ (3 nm)/γ-Al_2O_3 (1.5 nm) layer in which the Fe^{3+} and Co^{2+} oxidation states are observed.[17] These spectra may be measured through the γ-Al_2O_3 barrier since the escape depth of the electrons is about 5 nm. *In situ* AES was most useful in characterizing the oxidation state of the γ-Al_2O_3 film because of its chemical sensitivity to the existence of metallic Al. Figure 1(d) clearly shows the absence of any peak in the energy range corresponding to metallic Al, thus confirming that our crystalline aluminum oxide layer is indeed fully oxidized. It is important to note that there was no noticeable difference in the RHEED patterns or the XPS spectra for the $CoFe_2O_4$ barriers grown under different P_{O_2}.

For SPT measurements by the Meservey-Tedrow technique, a 4.2-nm-thick Al electrode was deposited on the Pt/$CoFe_2O_4$/γ-Al_2O_3 stack in a separate thermal evapora-

 ©2008 The American Physical Society

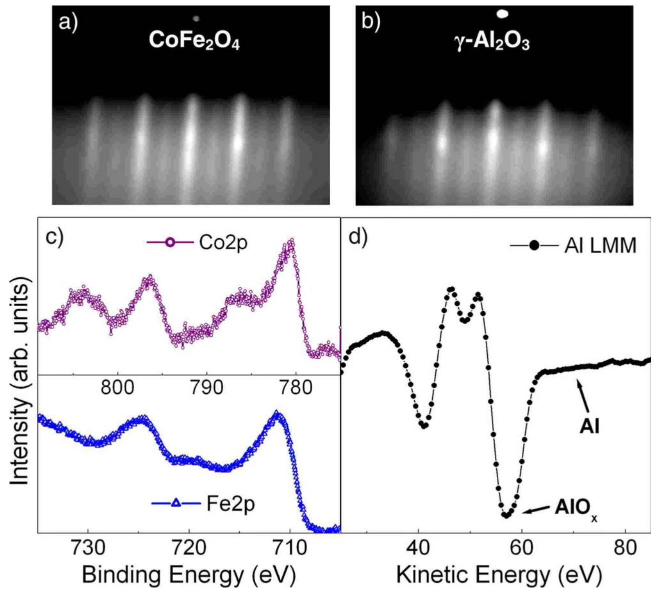

FIG. 1. (Color online) *In situ* structural and chemical analysis of a $CoFe_2O_4(111)$ (3 nm)/γ-$Al_2O_3(111)$ (1.5 nm) tunnel barrier including [(a) and (b)] the reflection high-energy electron-diffraction (RHEED) patterns along $[1\bar{1}00]$ and (c) the Co $2p$ and Fe $2p$ x-ray photoelectron spectroscopy (XPS) peaks. The Al *LMM* transition in the Auger electron spectroscopy (AES) spectrum of the γ-Al_2O_3 layer is shown in (d).

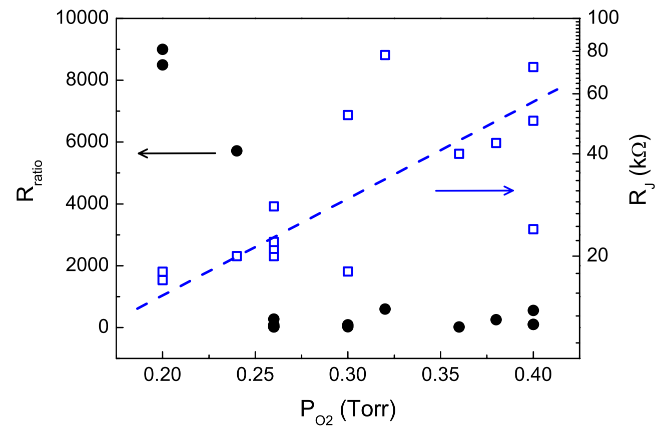

FIG. 2. (Color online) Tunnel junction temperature resistance ratio $[R_j(4\ \text{K})/R_j(300\ \text{K})]$ as a function of oxidation conditions for 15 junctions with P_{O_2}=0.2–0.4 Torr. The figure also shows the distribution of the junction resistances at 4 K, plotted in semilogarithmic scale, with the dotted blue line serving as a guide for the eyes.

tion chamber. Before beginning this process, the surface of the γ-Al_2O_3 layer was subjected to an oxygen plasma in order to minimize surface contamination from exposure to air. Next, an amorphous alumina definition layer was deposited from an electron-beam source, allowing us to define a long strip of $CoFe_2O_4$ with a simple shadow mask. Finally, the substrate was liquid-nitrogen cooled, and the 4.2 nm Al electrode was deposited as cross strips over the long strip to complete Pt/$CoFe_2O_4$/γ-Al_2O_3/Al tunnel junctions, whose area was approximately $500\times 150\ \mu m^2$.

Before performing SPT measurements, the resistance of each tunnel junction (R_j) was tracked during cooling from room temperature to 4 K. The increase in resistance, $R_{ratio}=R_j(4\ \text{K})/R_j(300\ \text{K})$, is plotted in Fig. 2 for a series of 15 junctions whose P_{O_2} during growth varied from 0.2 to 0.4 Torr. In this plot we immediately observe a substantial decrease in R_{ratio} for the junctions deposited with increasing P_{O_2} from 0.2 to 0.26 Torr, followed by a plateau or saturation beyond 0.26 Torr. The large R_{ratio} in the low-oxidized junctions is characteristic of a tunnel barrier containing point defects such as oxygen vacancies or chemical defects. In the present case, these are likely generated by oxygen vacancies in the lower-oxidized $CoFe_2O_4$ samples. This is evidence that oxygen vacancies influence the tunneling properties of our $CoFe_2O_4$ (3 nm)/γ-Al_2O_3 (1.5 nm) barriers. The point defects generate defect states in the band gap that act in lowering the effective barrier height of the tunneling electrons, and thus induce a stronger $R_j(T)$ dependence. Because they are associated with oxygen bands (*sp* type) that are expected to be weakly hybridized with the *d* bands from the Co and Fe, their exchange splitting should be weaker than that of the *d* states in the conduction band. One consequence of this could be a significant reduction in P_{SF}. Also, the probability of spin-scattering events due to the oxygen vacancies could increase, thus potentially influencing P_{SF} as well.

The evolution of the resistance values with increasing oxidation conditions also reveals a decrease in the number of defect states in the band gap for the higher-oxidized samples. This may be seen in the inset of Fig. 2, where the values at 4 K are plotted. The R_j values are somewhat scattered due to small deviations from the nominal barrier thickness from one junction to another. Even a variation of 0.1 nm in barrier thickness can considerably change R_j due to the exponential dependence of the tunneling current density on thickness. It is worth noting that the resistance increase is relatively small, compared to the increase in R_{ratio}, because the effect of defect levels is less dominant at low temperature. Also, because the R_{ratio} is self-normalized, it is a more reliable parameter than R_j alone. Nevertheless, there is a clear increasing trend in the $R_j(P_{O_2})$ distribution. This result again suggests that for the lower-oxidized samples, *sp*-type defect states in the band gap generated by oxygen vacancies lower the effective barrier height, thus lowering R_j.

SPT measurements were carried out next for the Pt (20 nm)/$CoFe_2O_4$ (3 nm)/γ-Al_2O_3 (1.5 nm)/Al (4.2 nm) tunnel junctions in a ^{3}He cryostat at 0.45 K, well below the critical superconducting temperature of the Al electrode (which we measured as 2.6 K). All samples with P_{O_2} ranging from 0.2 to 0.4 Torr were measured, but a variation in the SPT characteristics was observed only for samples grown between 0.2 and 0.26 Torr. We will therefore concentrate on the results from three sample sets with P_{O_2}=0.2, 0.24, and 0.26 Torr. The dynamic tunneling conductance (dI/dV) versus bias voltage (V) curves measured in all junctions at zero field showed zero conductance at V=0 and sharp symmetric peaks at ± 0.43 meV on either side of V=0. These properties confirm the high quality of the tunnel junctions. Upon application of a magnetic field, there was Zeeman splitting of the Al quasiparticle density of states (DOS). The Zeeman-split

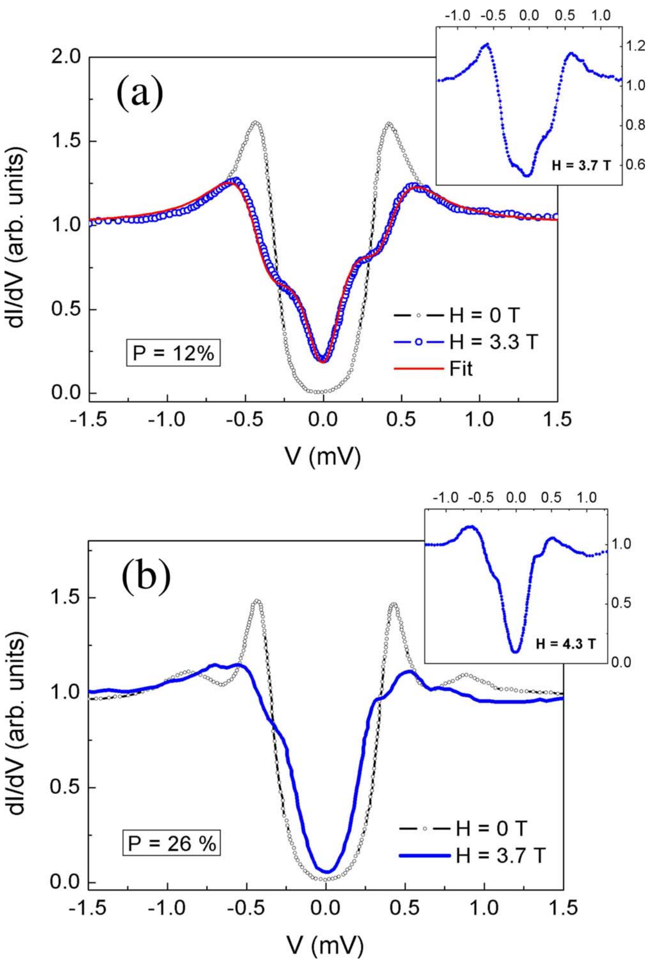

FIG. 3. (Color online) Spin-polarized tunneling in two Pt (20 nm)/$CoFe_2O_4$ (4 nm)/γ-Al_2O_3 (1.5 nm)/Al (4.2 nm) tunnel junctions grown in different oxidation conditions and measured at 0.45 K. (a) A 0.24 Torr sample measured at H=3.3 T and H=3.7 T (inset). (b) A higher-oxidized sample (0.26 Torr) measured at H=3.7 T and H=4.3 T (inset).

dI/dV curves were visibly asymmetric, indicating that the tunneling current is indeed spin polarized. In the 0.2 Torr sample (not shown), the asymmetry of the conductance peaks measured at 2.9 T corresponded to P_{SF}=6%.[4] Because there are no ferromagnetic electrodes in this structure, the polarization can only be explained by spin filtering in the $CoFe_2O_4$ barrier.

For the 0.24 Torr barrier, the asymmetry of the conductance peaks at H=3.3 and 3.7 T corresponds to P_{SF}=12%, shown in Fig. 3(a). We were able to obtain a more accurate value of P_{SF} by fitting them to the Maki-Fulde theory.[18] Briefly, the Maki-Fulde theory describes the DOS of a SC in an applied magnetic field taking into account the spin-orbit scattering (b) and orbital depairing (c). For the 0.24 Torr sample, the following values for the fitting parameters were used: T_c=2.8 K, T=0.45 K, H=3.31 T, b=0.03, c=0.08, and e_0=0.7, where e_0 is the Fermi-liquid parameter.[19] The result was P=12.5%, which agrees well with the value obtained by comparing the relative spin-up and spin-down peak heights,[4] thus justifying the exclusive use of this method to calculate P_{SF} from the dI/dV curves. The increased value of P_{SF} in the 0.24 Torr sample with respect to that for 0.2 Torr shows that the stronger oxidation conditions have a positive effect on the spin-filter efficiency of the $CoFe_2O_4$ barrier. This trend is further confirmed by the SPT measurement of the 0.26 Torr sample, which for an applied magnetic field of H=3.7 T yields P_{SF}=26% [Fig. 3(b)]. The small peaks at 0.88 meV are a consequence of the two-terminal method used for this particular sample and originate from the In-Al contacts. They do not change the deduced P_{SF}. Beyond P_{O_2}=0.26 Torr, no higher polarization was measured, indicating that the $CoFe_2O_4$ barriers reached saturation at this point.

The $R_j(T)$ and SPT results for the series Pt/$CoFe_2O_4$/γ-Al_2O_3/Al tunnel junctions described previously indicate that for $P_{O_2}<0.26$ Torr, the $CoFe_2O_4$ barriers contain enough defect states in the band gap due to oxygen vacancies to lower the spin-filter efficiency. The predominant *sp* character of these states makes them less sensitive to exchange splitting, thus explaining the reduction in P_{SF}. Above 0.26 Torr, no significant increase in P_{SF} was measured, in good agreement with the saturation of the temperature resistance ratio shown in Fig. 2, and suggesting that tunneling is dominated by the d states in the conduction band. One very important point is that the changes in oxygen vacancy concentration in our films grown in P_{O_2}=0.2 to 0.4 Torr were undetectable by all standard structural, chemical, and magnetic characterization techniques. Only the tunneling experiments were sensitive enough to detect an effect related to these minor defects.

The measurement of a non-negligible spin-filter effect is very encouraging, especially since this is a direct observation by the Meservey-Tedrow technique with a ferrite tunnel barrier. The positive sign of the measured P_{SF} is quite intriguing as this is neither consistent with the negative P_{SF} expected theoretically from band-structure calculations for the inverse and normal spinel structures,[14] nor with the negative TMR observed earlier in our Pt/$CoFe_2O_4$/γ-Al_2O_3/Co MTJs.[15] The Meservey-Tedrow technique being undoubtedly the most direct measurement of P in a tunneling current, this result is an indication of some additional factor, other than the DOS in the $CoFe_2O_4$ conduction band, influencing the overall mechanism for spin-polarized tunneling. The interpretation of this phenomenon is nontrivial, but in comparing the experimental conditions and samples used for the Meservey-Tedrow and TMR measurements, two main differences stand out. The first is the detector electrode, which is either Al or Co. The second is the bias voltage applied during the two tunneling experiments.

The measurement of an unexpected P has already been observed in Meservey-Tedrow experiments involving other systems. Most notably is the work of Thomas *et al.*[20] which measured positive P in Co/$SrTiO_3$/Al tunnel junctions, whereas TMR experiments on Co/$SrTiO_3$/$La_{2/3}Sr_{1/3}MnO_3$ MTJs already determined negative polarization in Co by De Teresa *et al.*[21] In the work of Thomas *et al.*,[20] one conjecture that they had was that the wave-function symmetry of the Al detector may actually determine the sign of P.

In the case of our Pt/$CoFe_2O_4$/γ-Al_2O_3/Al tunnel junctions, the effect of the Al detector electrode wave symmetry could be especially relevant if the alignment of the bands in the epitaxial barrier with those of the Al resulted in the preferential detection of the highly delocalized *sp* electrons, and thus positive *P*. This is more likely as electronic band-structure calculations show that *sp-d* hybridization in $CoFe_2O_4$ is weak.[14] The only structural difference between the tunnel junctions used for Meservey-Tedrow and TMR experiments being the detecting electrode (Al or Co, respectively), it is quite possible that the Al detector electrode wave symmetry is in fact responsible for the positive sign of *P* measured in the Meservey-Tedrow case.

The second main experimental difference between the Meservey-Tedrow and TMR experiments is the bias voltage used for the measurements. The SPT experiment is necessarily performed at very low bias (<2 mV) in order to probe the spin at the superconducting energy-gap region of the Al spin analyzer. In this bias-voltage regime, the direct-tunneling mechanism dominates, and the spin-dependent tunnel current densities ($J_{\uparrow(\downarrow)}$) are likely modified by the corresponding tunnel matrix elements.[22] In contrast, the TMR measurements were conducted at much higher voltages (50–200 mV). The TMR(V) curves showed that transport in this bias-voltage range was governed by Fowler-Nordheim tunneling, facilitated by the low tunnel barrier height of about 60 meV.[15] This indirect mechanism, different from that in the Meservey-Tedrow experiment, involves tunneling across the conduction band of the $CoFe_2O_4$ spin filter as it passes below the Fermi level.[23] As a result, it is expected that there will be spin accumulation at the $CoFe_2O_4/\gamma\text{-}Al_2O_3$ interface, which is necessarily negatively spin polarized because the DOS dominates here. Tunneling is thus a two-step process whose polarization should be determined by the DOS, ignoring the $\gamma\text{-}Al_2O_3$ tunnel matrix elements. The sign inversion of P_{SF} seen in the SPT result when compared to the TMR measurements may also be due to the bias voltage used for the two tunneling experiments, although the actual mechanism remains unclear.

In summary, we have demonstrated direct evidence of spin filtering in $CoFe_2O_4$ epitaxial tunnel barriers by the Meservey-Tedrow technique. SPT measurements of several $Pt/CoFe_2O_4/\gamma\text{-}Al_2O_3/Al$ tunnel junctions resulted in spin-filter efficiencies varying from 6% to 26%. The systematic increase in P_{SF} correlated directly with an increase in the oxidation conditions during the growth of the $CoFe_2O_4$. SPT results reveal that in the presence of oxygen vacancies, defect states in the $CoFe_2O_4$ band gap lower the effective tunnel barrier height, create spin-scattering centers, and are less exchange split, resulting in a reduction in the spin-filter efficiency. Finally, the measurement of the unexpected sign of *P* via the Meservey-Tedrow technique suggests that the tunneling mechanism in $CoFe_2O_4$ is not entirely governed by the DOS in the conduction band and that either the detector electrode wave-function symmetry or the bias-voltage regime, or both may have an important effect on the spin-filtering mechanism.

We wish to thank M. Gautier-Soyer for valuable discussions. We also acknowledge C. Deranlot for the growth of the Pt buffer layers. This work at MIT was supported by NSF and ONR grants as well as by the MIT-France program.

[1] R. Fiederling, M. Keim, G. Reuscher, W. Ossau, G. Schmidt, A. Waag, and L. W. Molenkamp, Nature (London) **402**, 787 (1999).
[2] J. S. Moodera, L. R. Kinder, T. M. Wong, and R. Meservey, Phys. Rev. Lett. **74**, 3273 (1995).
[3] D. P. DiVincenzo, J. Appl. Phys. **85**, 4785 (1999).
[4] R. Meservey and P. M. Tedrow, Phys. Rep. **238**, 173 (1994).
[5] J. S. Moodera, X. Hao, G. A. Gibson, and R. Meservey, Phys. Rev. Lett. **61**, 637 (1988).
[6] X. Hao, J. S. Moodera, and R. Meservey, Phys. Rev. B **42**, 8235 (1990).
[7] J. S. Moodera, R. Meservey, and X. Hao, Phys. Rev. Lett. **70**, 853 (1993).
[8] T. S. Santos and J. S. Moodera, Phys. Rev. B **69**, 241203(R) (2004).
[9] M. Gajek, M. Bibes, A. Barthélémy, K. Bouzehouane, S. Fusil, M. Varela, J. Fontcuberta, and A. Fert, Phys. Rev. B **72**, 020406(R) (2005).
[10] U. Luders, M. Bibes, K. Bouzehouane, E. Jacquet, J.-P. Contour, S. Fusil, J. Fontcuberta, A. Barthélémy, and A. Fert, Appl. Phys. Lett. **88**, 082505 (2006).
[11] B. B. Nelson-Cheeseman, R. V. Chopdekar, L. M. B. Alldredge, J. S. Bettinger, E. Arenholz, and Y. Suzuki, Phys. Rev. B **76**, 220410(R) (2007).
[12] P. LeClair, J. K. Ha, J. M. Swagten, J. T. Kohlhepp, C. H. van de Vin, and W. J. M. de Jonge, Appl. Phys. Lett. **80**, 625 (2002).
[13] M. G. Chapline and S. X. Wang, Phys. Rev. B **74**, 014418 (2006).
[14] Z. Szotek, W. M. Temmerman, D. Kodderitzsch, A. Svane, L. Petit, and H. Winter, Phys. Rev. B **74**, 174431 (2006).
[15] A. V. Ramos, M.-J. Guittet, J.-B. Moussy, R. Mattana, C. Deranlot, F. Petroff, and C. Gatel, Appl. Phys. Lett. **91**, 122107 (2007).
[16] M. Jullière, Phys. Lett. A **54**, 225 (1975).
[17] S. A. Chambers, R. F. C. Farrow, S. Maat, M. F. Toney, L. Folks, J. G. Catalano, T. P. Trainor, and G. E. Brown, Jr., J. Magn. Magn. Mater. **246**, 124 (2002).
[18] K. Maki, *Superconductivity* (Marcel Dekker, New York, 1969), Vol. 2.
[19] G. A. Gibson, P. M. Tedrow, and R. Meservey, Phys. Rev. B **40**, 137 (1989).
[20] A. Thomas, J. S. Moodera, and B. Satpati, J. Appl. Phys. **97**, 10C908 (2005).
[21] J. M. De Teresa, A. Barthélémy, A. Fert, J.-P. Contour, F. Montaigne, and P. Seneor, Science **286**, 507 (1999).
[22] I. I. Mazin, Phys. Rev. Lett. **83**, 1427 (1999).
[23] T. Nagahama, T. S. Santos, and J. S. Moodera, Phys. Rev. Lett. **99**, 016602 (2007).